Clin Neuroradiol
https://doi.org/10.1007/s00062-019-00871-4

REVIEW ARTICLE

Blake's Pouch Cysts and Differential Diagnoses in Prenatal and Postnatal MRI

A Pictorial Review

Thomas Kau[1,2] · Robert Marterer[2] · Raimund Kottke[3] · Robert Birnbacher[4] · Janos Gellen[5,6] · Eszter Nagy[2] · Eugen Boltshauser[7]

Received: 22 October 2019 / Accepted: 16 December 2019

Abstract

Purpose The clinical variability of Blake's pouch cysts (BPC) may range from asymptomatic via ataxia to sequelae of decompensated hydrocephalus. On the other hand, Dandy-Walker malformation (DWM) and cerebellar vermis hypoplasia generally correlate with less favorable neurologic development. The aim was to illustrate the potential of prenatal and postnatal neuroimaging to distinguish a BPC or persistent BP from other posterior fossa malformations.

Methods This pictorial review addresses the inconsistent nomenclature, clinical features, and magnetic resonance imaging (MRI) patterns of BPC and five differential diagnoses. The MRI findings of 11 patients, acquired at up to 3 T in 3 institutions, are demonstrated. Furthermore, the literature was searched for recent improvements in genetic and embryological background knowledge.

Results Posterior fossa malformations often resemble each other and may even be imitated by sequelae of hemorrhagic, ischemic or infectious disruptions, i.e. congenital anomalies of morphology despite normal developmental potential. Hydrocephalus is a typical, albeit not always congenital finding in BPC. It is frequently associated with cerebellar disruptions and DWM; however, it is also a rare complication of posterior fossa arachnoid cysts. A moderately elevated vermis needs follow-up to confirm persistent BP versus vermian hypoplasia or DWM. The fetal cerebellar tail, previously assumed to be specific for DWM, may be imitated in cases of persistent BP.

Conclusion The accurate diagnosis of isolated BPC is not always straightforward, which is especially critical in the context of fetomaternal medicine. A detailed description of posterior fossa malformations is to be preferred over unspecific terminology.

Keywords Arachnoid cyst · Mega cisterna magna · Cerebellar hypoplasia · Dandy-Walker malformation · Cerebellar disruption

Author Contributions T. Kau had the idea for this article, performed literature search, provided data, and drafted the article, E. Boltshauser performed literature search, provided data, and critically revised the article, R. Kottke provided data and critically revised the article, R. Marterer, R. Birnbacher, J. Gellen and E. Nagy commented on the data and critically revised the manuscript.

✉ Thomas Kau
thomas.kau@kabeg.at

[1] Institute of Radiology, Villach General Hospital, Villach, Austria

[2] Division of Pediatric Radiology, Department of Radiology, Medical University of Graz, Graz, Austria

[3] Section of Neuroradiology, Department of Diagnostic Imaging and Intervention, University Children's Hospital Zurich, Zurich, Switzerland

[4] Department of Pediatrics and Adolescent Medicine, Villach General Hospital, Villach, Austria

[5] Division of Obstetrics and Maternal Fetal Medicine, Department of Gynecology and Obstetrics, Medical University of Graz, Graz, Austria

[6] Department of Gynecology and Obstetrics, Villach General Hospital, Villach, Austria

[7] Department of Pediatric Neurology, University Children's Hospital Zurich, Zurich, Switzerland

Published online: 15 January 2020

Purpose

While about 90% of fetuses with either isolated Blake's pouch cysts (BPC) or mega cisterna magna (MCM) are reported to have normal developmental outcome, Dandy-Walker malformation (DWM) and hypoplasia of the cerebellar vermis correlate with less favorable neurologic development in a high percentage of cases [1, 2]. This article aims to illustrate the potential of magnetic resonance imaging (MRI) to distinguish a BPC or persistent BP from several differential diagnoses in the fetal period and during childhood.

Blake's Pouch Cysts

Blake's pouch cysts (BPC), first appreciated as a separate entity by Tortori-Donati et al. in 1996 [3], represents a midline cystic malformation of the posterior fossa [4]. It is attributed to absent fenestration of BP, an embryological expansion of the posterior membranous area continuous with the fourth ventricle [3, 4]. The infracerebellar or infraretrocerebellar cyst is associated with a lack of communication between the fourth ventricle and the subarachnoid space, as also shown by phase-contrast studies [5, 6]. In a recent study of transvaginal ultrasound in 67 pregnant women, the fourth ventricular choroid plexus was "down" relative to the roof of the fourth ventricle in all cases of DWM and vermian hypoplasia (VH), while it was "up" in all cases of BPC at a mean gestational age of nearly 24 weeks [7]. Displacement of the choroid plexus to the superior cyst wall is not consistently visible in clinical MRI [8]. A BPC typically leads to tetraventricular hydrocephalus (Fig. 1; [3, 9]). Usually, BPs communicate with the subarachnoid space by 18 weeks gestation to form the foramen of Magendie [4, 10]. In the case of non-perforation, all four ventricles will enlarge until the foramina of Luschka open (Fig. 1) and establish a labile equilibrium of cerebrospinal fluid (CSF) between the ventricles and the cisterns [11].

With persistent BP, the cerebellar hemispheres and the variably elevated vermis tend to be compressed and displaced rather than hypoplastic (Fig. 1; [10, 12]). Delayed vermian rotation may be a pitfall in prenatal imaging (Fig. 2) and a potential risk of unnecessary pregnancy interruption [13]. Follow-up in the early third trimester is recommended (Fig. 2; [12, 13]). Fetal MRI, which is believed to be safe within accepted specific absorption rate (SAR) limits at 1.5 T and 3 T, plays an important role in the classification of posterior fossa malformations; however, the discrimination of mild hypoplasia from slight deformation of the cerebellar vermis remains challenging in fetal and even postnatal high-field MRI (Fig. 2; [12]).

The clinical and morphological variability of BPC is not sufficiently documented. According to the literature, it may range from asymptomatic via ataxia or vertigo to sequelae of decompensated hydrocephalus [14, 15]. Late onset and even a secondary form with re-expanding BP remnants have been described [15, 16]. Treatment of symptomatic BPC is surgical and the placement of a ventriculoperitoneal (VP) shunt a well-established method [14]; however, endoscopic

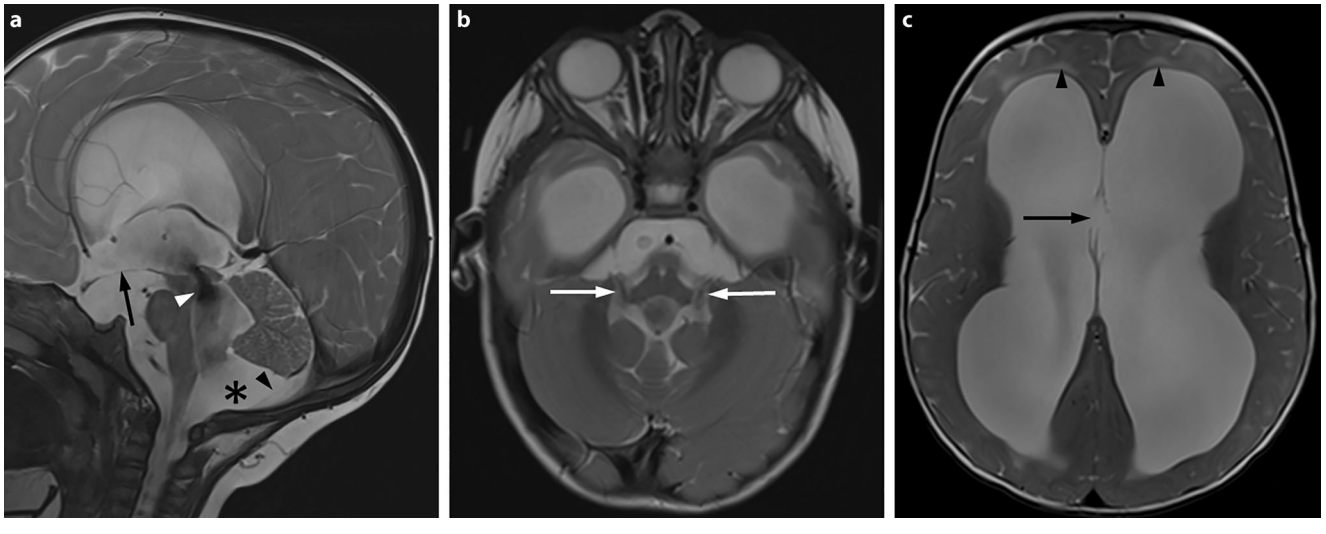

Fig. 1 **a–c** Preoperative T2-weighted 3 T magnetic resonance (MR) imaging in a 9-month-old female infant with severe tetraventricular hydrocephalus. **a** Marked flow void (*white arrowhead*) in an open Sylvian aqueduct and turbulent dephasing between the widened fourth ventricle and Blake's pouch cyst (*asterisk*) are demonstrated in the sagittal image. The thin posterior cyst wall (*black arrowhead*) can be delineated inferior to the slightly elevated and compressed posterior vermian lobe. **b** The foramina of Luschka (*arrows*) are open as inferred from symmetrical flow voids in axial MR images. This has established a delicate equilibrium of cerebrospinal fluid outflow from the ventricles into the cisterns leading to concavity of the floor of the third ventricle (**a**, *arrow*). **c** Hydrocephalus is associated with periventricular interstitial edema (*arrowheads*) indicating increased intracranial pressure in this axial slice at the level of the perforated septum pellucidum (*arrow*)

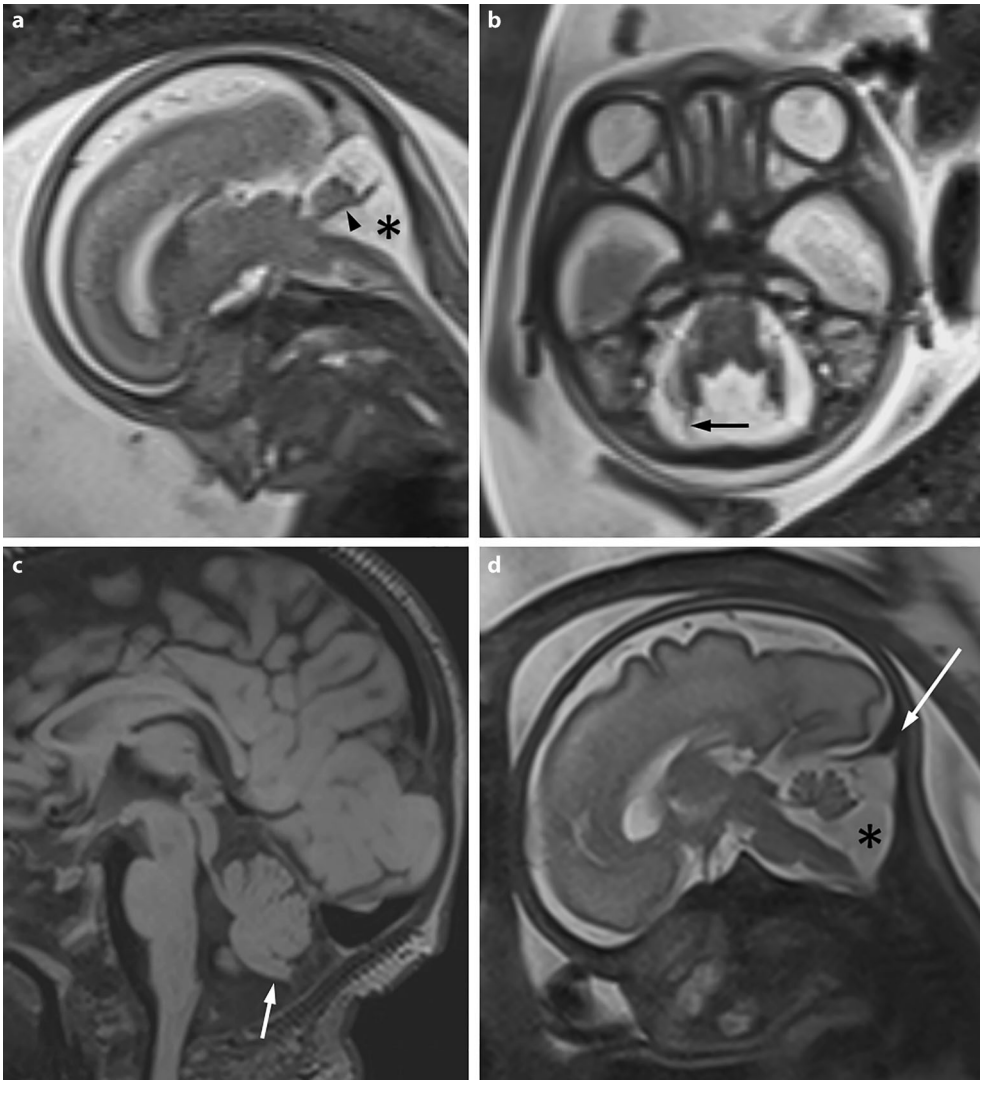

Fig. 2 Slightly off midline sagittal (**a**) and axial (**b**) half-Fourier acquisition single-shot turbo spin-echo (HASTE) T2-weighted 3 T magnetic resonance images of the fetal brain at 21 weeks gestation suggesting a slightly hypoplastic cerebellar vermis with the fastigial point flattened (**a** *arrowhead*) and a moderately increased tegmento-vermian angle of about 35°. A lateral septum (**b** *arrow*) in the posterior fossa is considered to belong to Blake's pouch (**a** *asterisk*). The follow-up HASTE image derived from the same scanner at 31 weeks gestation shows nearly normal rotation of the vermis in a slightly enlarged posterior fossa (**c** *asterisk*) suggesting delayed fenestration of Blake's pouch. Normal torcular position (**c** *arrow*) is confirmed. Mild inferoposterior vermian hypoplasia may be suspected from early third trimester gestational imaging. A similar pattern is depicted after birth on a sagittal fluid-attenuated inversion recovery (FLAIR) image (**d**) acquired at the age of 12 weeks. Size and shape of the cerebellar vermis imply mild hypoplasia and that its posterior lobe (**d**, *arrow*) has experienced mass effect due to prolonged persistence of Blake's pouch

third ventriculostomy is less invasive and has been advocated as the preferred treatment option by some authors [15, 17]. Fenestration of the cyst may be an insufficient treatment with a higher risk for complications, as previously reported [14].

Posterior Fossa Arachnoid Cyst

Arachnoid cysts (AC) are lesions filled with cerebrospinal fluid (CSF) lined by the arachnoid membrane that do not communicate with the neighboring subarachnoid space or ventricles [8]. Frequently, they are found posterior or inferior to the vermis but can be located in any positional relationship to the cerebellum (Fig. 3; [18]). The computed tomography density and MRI signal characteristics are equivalent to that of CSF (Fig. 4). Follow-up imaging every 2 weeks has been recommended for posterior fossa AC detected in the fetal period to evaluate its growth and space-occupying effect [19].

Albeit not typically associated with hydrocephalus, AC may cause a mass effect depending on size and location. Increased intracranial pressure and neurodevelopmental impairment have been associated with AC [8]; however, most posterior fossa AC are asymptomatic and surgery is rarely needed. In a long-term study of symptomatic posterior fossa AC shunted in infancy, the authors found a favorable prognosis for cognitive development and neurological signs [18].

Mega Cisterna Magna

Just like BPC, MCM has traditionally been associated with an embryological defect of the posterior membranous area resulting in late fenestration of BP [3]. Incremental importance is now attributed to the meninges for the develop-

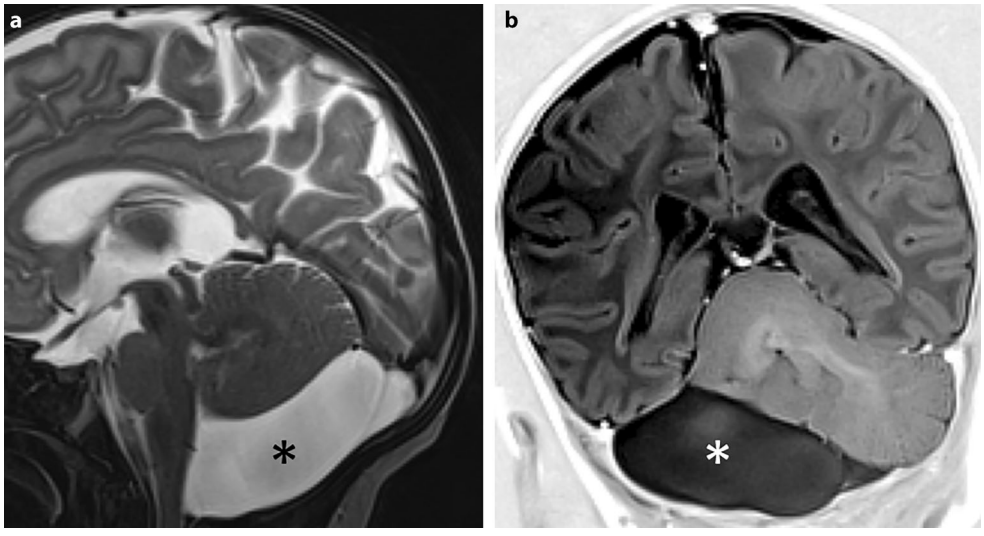

Fig. 3 **a**, **b** Mid-sagittal T2-weighted turbo spin echo (TSE) (**a**) and coronal triple inversion recovery (TIR) sequence (**b**) images from 1.5 T magnetic resonance imaging in a 2-month-old female patient scanned for a posterior fossa cyst incidentally found by sonography on the first day of life. The *asterisks* indicate a space-occupying infracerebellar arachnoid cyst. Besides being asymmetrically compressed and slightly elevated, the cerebellum appears normal in structure. The overlying skull shows thinning and scalloping. Within a follow-up period of 5 years, the girl showed normal neurological development

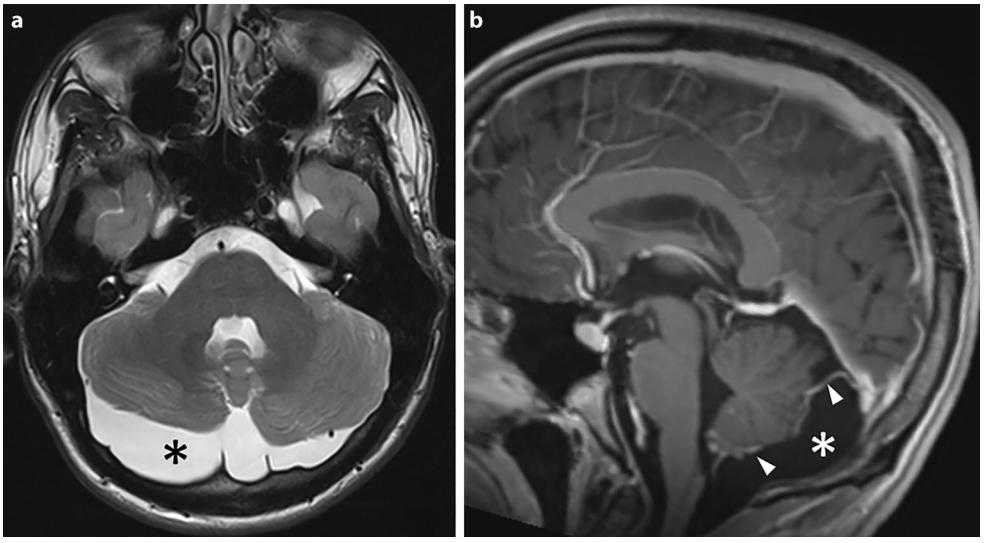

Fig. 4 **a**, **b** 3 T magnetic resonance (MR) imaging of the brain in an 18-year-old male patient scanned for posttraumatic brain lesions. The axial T2-weighted MR image (**a**) and the contrast-enhanced 3D magnetization-prepared rapid gradient-echo (MP-RAGE) image (**b**) depict a normal shaped fourth ventricle and a retrocerebellar cystic structure (*asterisks*) with small veins (*arrowheads*) running along its periphery. The incidental finding in the posterior fossa is compatible with an arachnoid cyst

ing cerebellum as also shown by animal models [20, 21]. The MCM represents a variably enlarged cisterna magna (≥10 mm on midsagittal images) with a normal brain stem and cerebellum (Fig. 5; [8]). The latter favors the diagnosis of MCM compared to AC. The concept of MCM being a cystic malformation is controversial. Due to free communication with the fourth ventricle and spinal subarachnoidal space, it does not lead to hydrocephalus [9]. There is broad acceptance that MCM is an incidental finding and per se associated with a good prognosis; however, it has also been described in association with human filamin A gene mutations along with classical X-linked bilateral periventricular nodular heterotopia, cardiovascular malformations and epilepsy [22, 23].

Cerebellar and Vermian Hypoplasia

Cerebellar hypoplasia (CH) is a nonspecific descriptive term referring to reduced volume of the cerebellum [24]. For the purpose of precise evaluation both in MRI and sonography, biometric reference data have been published for the developing vermis and posterior fossa [7, 25–27]. Neuroimaging provides key information for the categorization of congenital cerebellar abnormalities which may be due to malfor-

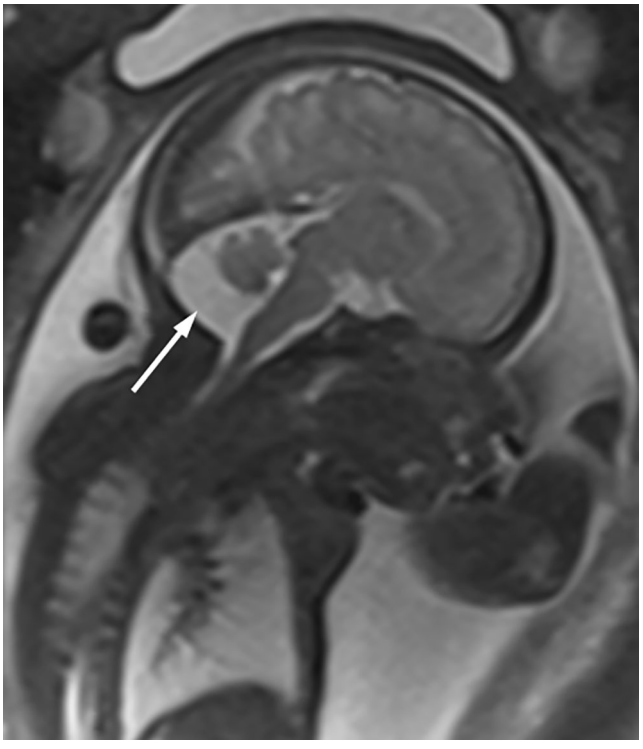

Fig. 5 Mid-sagittal half-Fourier acquisition single-shot turbo spin-echo (HASTE) image from 3 T magnetic resonance imaging of the fetal brain at 33 weeks gestation. The enlarged cerebrospinal fluid space (*arrow*) posterior and inferior to a normal cerebellar vermis in the absence of hydrocephalus suggests mega cisterna magna

mation (primary) or disruption (secondary) [8, 28]. It is crucial to differentiate the variable etiologies in terms of prognosis and genetic counseling. Reliable fetal MRI of the cerebellum starts from 19 to 20 weeks of gestation [24, 28]. Primary conditions include chromosomal aberrations, metabolic disorders, genetic syndromes (e.g. Joubert), and other brain malformations (e.g., Dandy-Walker) [8]. Inducing and maintaining the basal lamina and glia limitans, the meninges are essential for a normal cerebellar development. Remarkably, heterozygous mutations of *FOXC1* which encodes a transcription factor expressed by meningeal cells are accompanied by VH [21].

Somatic mutations have been proposed for the PHACE association consisting of posterior fossa anomalies, hemangioma, arterial anomalies, cardiac anomalies, and eye anomalies [29]. This genetic association comprises posterior fossa anomalies, hemangioma, arterial anomalies, cardiac anomalies and eye anomalies [30]. In the fetal period, the cerebellar "tilted telephone receiver sign" is believed to be a specific imaging feature of PHACE(S) [31]. Unilateral CH with occasional involvement of the cerebellar vermis (Fig. 6) has to be expected in PHACE(S) patients with affection of the posterior fossa [30]. In contrast, DWM is infrequently associated with PHACE(S) [30].

The "molar tooth sign" is a pathognomonic feature of Joubert syndrome, an autosomal recessive ciliopathy with the exception of *OFD1* mutation which is X-linked. It is accompanied by hypoplasia or dysplasia of the cerebellar vermis (Fig. 7; [32]). This imaging pattern is composed of thickened, elongated, and horizontally orientated superior cerebellar peduncles with an abnormally deep interpeduncular fossa [30]. Ultimately, Joubert syndrome comprises a wide spectrum of imaging findings. Morphology may rather predict the neurodevelopmental outcome than the genetic cause [33], i.e. VH of a higher grade tends to correlate with worse neurodevelopmental outcome. More than 40 genes are currently known to be associated with Joubert syndrome.

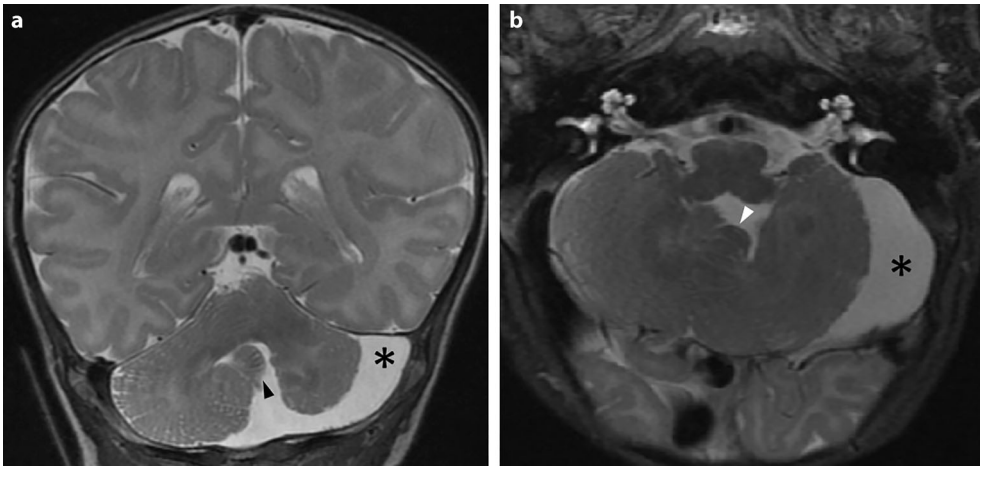

Fig. 6 **a**, **b** Coronal (**a**) and axial (**b**) T2-weighted fast spin-echo (FSE) images of the brain in a 3-week-old patient depicting an abnormal vermis (*arrowheads*) and left-sided cerebellar hypoplasia with pronounced cerebrospinal fluid (CSF) space (*asterisks*). The cerebellum is dysplastic with cortical anomaly and areas of heterotopia throughout the cerebellar white matter. Associated ipsilateral hemangioma of the head and absence of the internal carotid artery are not shown. This constellation is characteristic for PHACE association

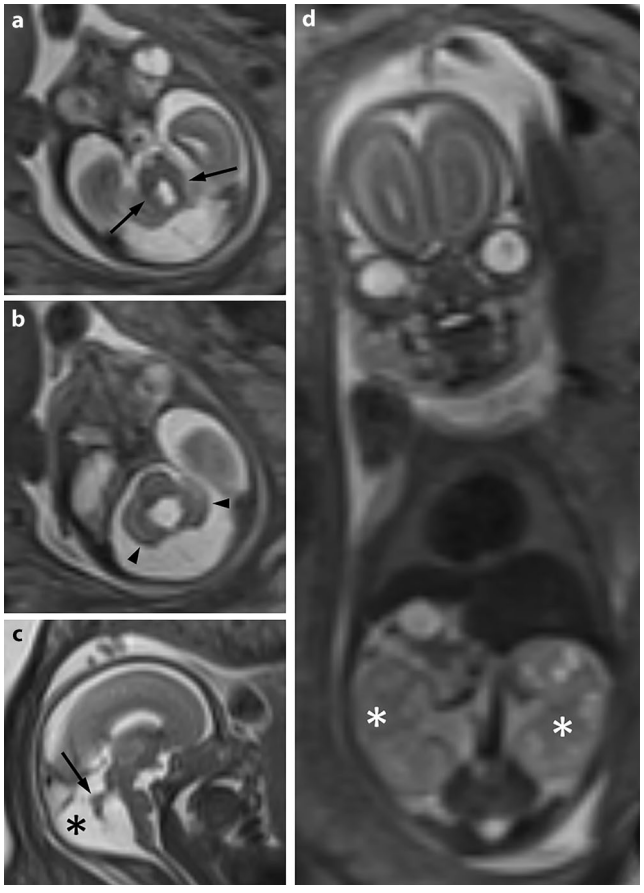

Fig. 7 **a**–**d** Fetal 3 T magnetic resonance imaging at 20 weeks gestation following sonographic suspicion of persistent Blake's pouch. Thickened, elongated, and horizontally orientated superior cerebellar peduncles (**a**, *arrows*) compatible with "molar tooth sign", roughly normal cerebellar hemispheres (**b**, *arrowheads*), an enlarged posterior fossa (**c**, *asterisk*), and a hypoplastic, moderately elevated vermis (**c**, *arrow*) are shown in axial (**a**, **b**) and sagittal (**c**) HASTE images. The association with enlarged polycystic kidneys (**d**, *asterisks*), as depicted on a coronal HASTE image, suggests a cerebellorenal phenotype within the Joubert syndrome spectrum

Cerebellar dysplasia (CD), defined as abnormal cerebellar foliation and fissuration, white matter arborization, and abnormal grey-white matter junction has been described in the context of few posterior fossa malformations with recessive inheritance [8, 24]. Cortical CD without cysts is suggestive of tubulinopathies, a group of heterozygous disorders further characterized by cortical, basal ganglia and commissural malformations and invariably associated with intellectual disability [34]. They have to be distinguished from other autosomal recessive disorders with CD associated with different clinical features such as hearing loss (Chudley-McCullough syndrome), retinal dystrophy (Poretti-Boltshauser syndrome), muscular dystrophy (dystroglycanopathies) and progressive retinal, kidney and liver disease (Joubert syndrome). Focal CD may also be found in unilateral cerebellar cleft or hypoplasia on the basis of prenatal cerebellar disruptions [24, 34]. Secondary causes of CH include prenatal infections, exposure to teratogens, and extreme prematurity [8].

Despite limitations in the ability to distinguish it from persistent BP with putative compression of the vermis, the term "inferior VH" is increasingly used [10, 13, 35]. If at all VH coexists with BPC, with respect to its ventral to dorsal development it may not necessarily be the inferior vermis that is abnormal [12, 35]. The position of the choroid plexus has been suggested to be a discriminator between true VH and BPC [9, 35]. According to an early fetal MRI study performed on a 1.5 T scanner, suspected isolated inferior VH in second trimester imaging was confirmed postnatally in less than 70% of cases [36]. Despite a tendency towards lower behavioral and functional scores as compared to normal controls, the developmental outcome of infants with confirmed inferior VH was reported to be overall good [36]. It has to be kept in mind that even after postnatal revision based on imaging and clinical tests, the prenatal diagnosis

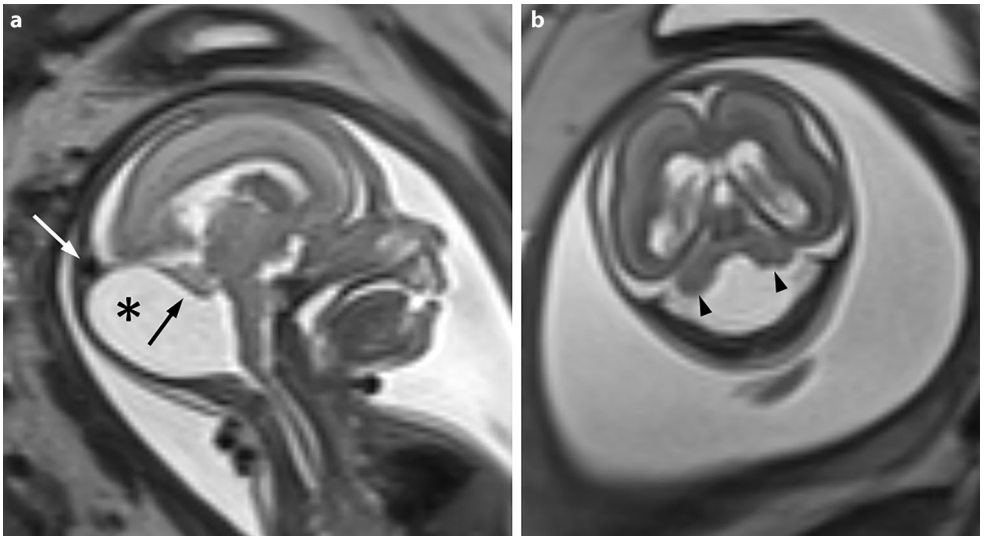

Fig. 8 Mid-sagittal (**a**) and coronal (**b**) HASTE 3 T magnetic resonance images of the fetal brain at 23 weeks gestation. **a** Cystoid dilatation of the fourth ventricle in an enlarged posterior fossa (*asterisk*) is associated with elevation of the hypoplastic cerebellar vermis (*black arrow*) and the torcula (*white arrow*). The tegmento-vermian angle (130°) is markedly increased. **b** Moderately displaced cerebellar hemispheres (*arrowheads*) appear normal in shape and size. The findings are compatible with Dandy-Walker malformation

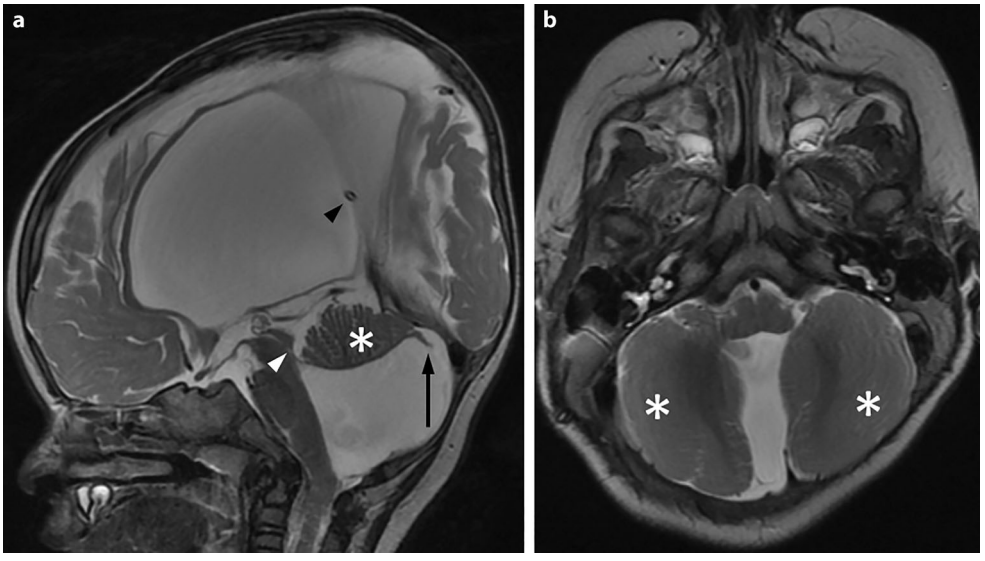

Fig. 9 Mid-sagittal (**a**) and axial (**b**) T2-weighted fast spin-echo (FSE) images of the brain in a 9-month-old patient after shunt (**a**, *black arrowhead*) placement for chronic hydrocephalus in the context of Dandy-Walker malformation. **a** Occlusion of the Sylvian aqueduct (*white arrowhead*) with absent flow void has developed postnatally. Configuration of the folia and lobules of the anterior lobe and the upper portion of the posterior lobe of the vermis (*asterisk*) is approximately normal. The lower portion of the posterior lobe is almost completely missing and in continuity with a "tail" (*arrow*) that possibly represents ependyma and connective tissue of the extremely enlarged fourth ventricular roof. **b** The cerebellar hemispheres (*asterisks*) appear normal in size and structure

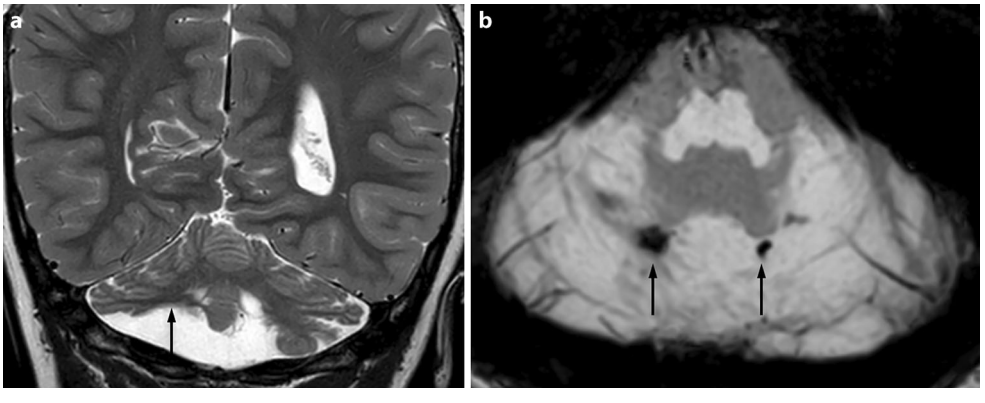

Fig. 10 **a**, **b** Magnetic resonance images of the brain in an 8-year-old female patient of short stature primarily sent for evaluation of the pituitary gland. The coronal T2-weighted turbo spin echo (TSE) image depicts irregular volume reduction at the base of both cerebellar hemispheres with right-sided predominance (**a**, *arrow*). The axial susceptibility-weighted image (SWI) shows bilateral focal signal loss (**b**, *arrows*) posterior to the lateral recess of the enlarged fourth ventricle, most likely representing hemosiderin deposits. The imaging pattern is compatible with cerebellar disruption due to hemorrhage

of VH may be associated with a persistently elevated level of parental stress.

Dandy-Walker Malformation

The DWM, initially described by Dandy and Blackfan in 1914 [37], is defined by hypoplasia, elevation, and counterclockwise upward rotation of the cerebellar vermis, cystic dilatation of the fourth ventricle extending posteriorly into the enlarged posterior fossa (Fig. 8; [8, 28, 38]). Elevation of the tentorium and torcula (torcula-lambdoid inversion) is commonly associated but not a consistent finding and therefore not included in the diagnostic criteria [8]. The same is true for hydrocephalus. The prevalence of DWM as an isolated malformation has been reported to be 1 in 30,000 live births and the risk of recurrence is low [8].

The embryological concept of BPC and MCM originating from a defect of the posterior membranous area and DWM from a defect of the anterior membranous area is nowadays regarded as simplistic [3, 20, 21, 39]. In mice, the *FOXC1* gene which encodes a transcription factor expressed by meningeal cells plays a crucial role in cerebellar development [21]. Posterior fossa malformations ranging

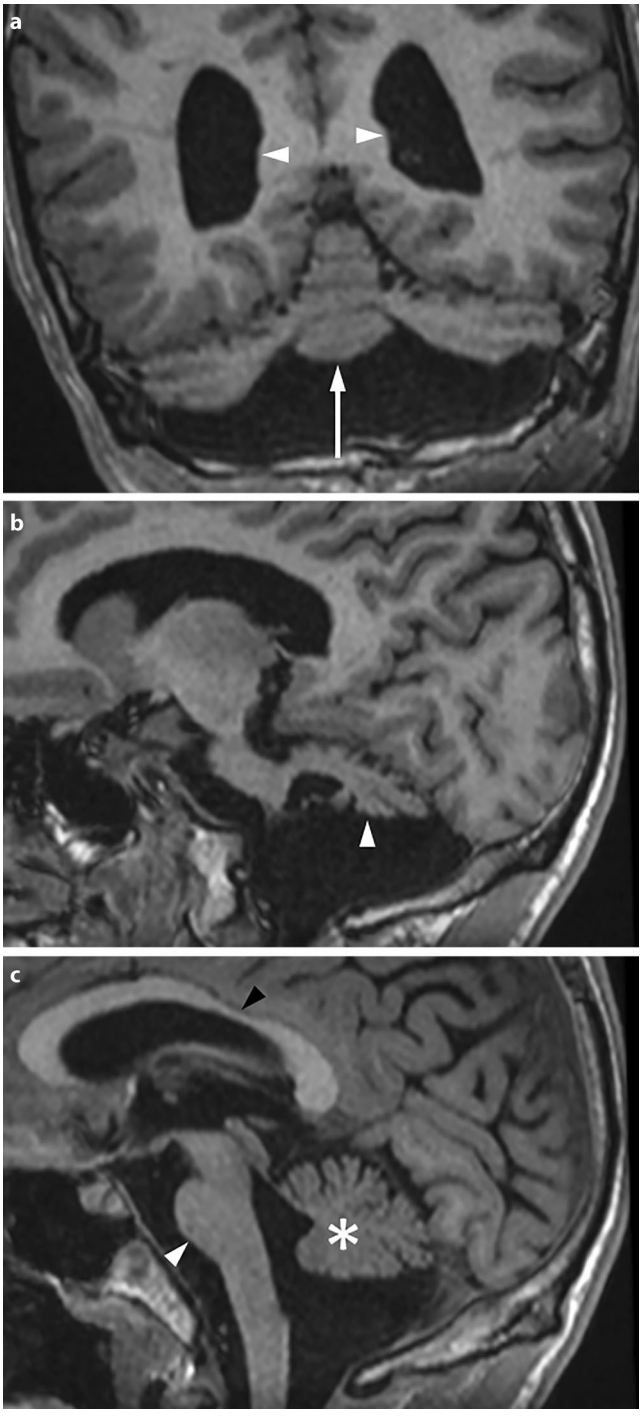

Fig. 11 **a**–**c** T1-weighted gradient echo sequence images in a 17-year-old patient with a history of cerebellar disruption following extreme prematurity. Emergency cesarean section was performed at 27 weeks gestational age. **a** The coronal image shows cerebellar hypoplasia with the vermis (*arrow*) being less affected, therefore leading to a "dragonfly pattern". Mild colpocephaly (*arrowheads*) is the result of periventricular leukomalacia. **b** A sagittal slice through the superior cerebellar peduncle depicts marked hypoplasia of the cerebellar hemisphere (*arrowhead*). **c** The mid-sagittal image shows the vermis (*asterisk*) to be relatively preserved. The pontine protuberance (*white arrowhead*) appears reduced and an exceptionally pronounced callosal isthmus (*black arrowhead*) reflects some white matter loss

from MCM to DWM are a near-constant finding in single allele deletion of *FOXC1* gene affecting the p25.3 region of chromosome 6 in humans [21, 40]. Importantly, DWM in the narrow sense does not seem to be due to the sole haploinsufficiency of *FOXC1* [20].

Despite important clinical distinctions, several genes have been associated both with CH subtypes and with DWM suggesting that these entities may each represent one end of a wide spectrum [41]. Not only have many key mechanisms controlling cerebellar development been preserved between mouse and human, but also the partially formed posterior lobule in hypomorphic *FOXC1* mutant mice has been shown to resemble the neuroradiological "tail sign" observed in human DWM [40]. Based on a retrospective study of 31 fetal MRI examinations including one Blake's pouch cyst, four "vermian malrotations", and 15 DWM cases, Bernardo et al. referred to the Dandy-Walker tail as a specific marker for DWM [42]. Indeed, there is a pathoanatomical equivalent that represents an underdeveloped posterior vermian lobule in continuation with a membrane consisting of ependyma and connective tissue [43]. It has recently been shown in a small number of cases that the molecular diagnostic rate is even lower in DWM with what has been called "unpaired caudal lobule" compared to DWM without this tail [41]. With respect to a case of delayed rupture of Blake pouch (Fig. 2), there are concerns about the specificity of this neuroradiological sign (Fig. 9). In our opinion, it may be misleading only because there is no unequivocal imaging correlate for a "tail" in the context of posterior fossa malformations. Furthermore, since terms like Dandy-Walker variant, complex or spectrum lack specificity and sometimes cause confusion, a detailed description of the imaging pattern is to be preferred [8, 28]. The semantic dilemma may arise with a variably abnormal vermis, inconsistent size of the CSF space, and difficulty in relating the torcular level to the lambdoid [38].

In the context of DWM, VH consistently affects the inferior part. The cerebellar hemispheres, typically displaced anterolaterally, may be normal in size and shape, hypoplastic and/or dysplastic (Fig. 8; [8]). In contrast to BP (Fig. 2a) or isolated VH, the tegmento-vermian angle is >45° in DWM (Fig. 8; [8, 44]). In severe cases, the vermis may become attached to the tentorium or even be absent. Despite being a frequent complication, hydrocephalus is not usually present at birth and, therefore, not a constant part of the malformation [45]. The inconsistent presence and degree of communicating hydrocephalus is more due to a variable patency of the foramina of Luschka and Magendie [8]. The brain stem may or may not appear thin [8]. Once the prenatal diagnosis of DWM is suspected during the second trimester, associated supratentorial malforma-

Table 1 Key neuroimaging features of BPC and its differential diagnoses

Malformation	Posterior Fossa	Vermis	Cerebellar "tail sign"	Tegmento-vermian Angle	Fourth Ventricle	Hydrocephalus	Torcula
BPC	Normal	Normal	Possible	Usually <30°	Enlarged	Very frequent	Normal
AC	Normal	Normal	No	Normal	Normal or reduced	Rare	Normal
MCM	Inconsistently enlarged	Normal	No	Normal	Normal	No	Normal
CH/VH	Normal	Hypoplastic	No	Usually 30–45° in VH	Enlarged	No	Normal
DWM	Enlarged	Hypoplastic	Yes	>45°	Enlarged	Frequent	Elevated
CD	Normal	Normal or reduced	No	Normal or enlarged	Enlarged	Occasional	Normal

BPC Blake's pouch cyst; *AC* arachnoid cyst; *MCM* mega cistern magna; *CH/VH* cerebellar hypoplasia/vermian hypoplasia; *DWM* Dandy-Walker malformation; *CD* cerebellar disruption [37, 51]

tions have to be taken into account for the estimation of cognitive outcome.

A DWM may occur isolated or as part of a Mendelian syndrome, aneuploidies, or other chromosomal abnormalities [8]. Macrocephaly is very common and the majority of affected children present with signs of increased intracranial pressure within their first year of life [8]. Muscular hypotonia and developmental delay are frequent features, while ataxia and nystagmus present in half of the patients, typically later in life [8]. At least one third of children with DWM show normal cognitive development [8, 46]. Normal vermian lobulation and exclusion of associated abnormalities, such as callosal dysgenesis have been reported to be favorable factors [47].

Cerebellar Disruptions

Disruption in this context is defined as a congenital morphological defect resulting from an extrinsic breakdown of originally normally developed tissue [24]. Malformative hypoplasia of the cerebellum or, more specifically, of the vermis may be imitated by the morphologic sequelae of a disruptive event such as prenatal infection (in particular cytomegalovirus and Zika virus), hemorrhage, or ischemia [24, 36]. Thus, in cases of cerebellar disruption, the affected structure shows a congenital anomaly in size and shape despite its normal developmental potential [24].

According to a large retrospective MRI study, isolated cerebellar hemorrhagic lesions occur within the first two trimesters with a prevalent origin peripherally or caudally in the hemispheres and either unilateral or bilateral involvement ([48]; Fig. 10). Symmetric volume reduction of the cerebellum may also occur as a consequence of extreme prematurity ([49]; Fig. 11). In combination with perinatal risk factors, such as hemosiderin deposition, this selective vulnerability often leads to parenchymal destruction and arrested development [50]. Ontogenetically, the germinal matrix of the cerebellum is located in highly vascularized regions both adjacent to the fourth ventricle and in the external granular layer. Perinatal factors that increase the risk for supratentorial intraventricular hemorrhage also play a role in the cerebellum [51].

Long-term outcome will most probably differ between cases of primary dysgenetic versus acquired disruptions, albeit there is a lack of evidence for this suggestion [24]. Disruptions are acquired lesions with very low recurrence risk, although a genetic predisposition may be present [24, 52].

Conclusion

A neuroradiologist confronted with a case of supposed BPC is facing two dilemmas: First, posterior fossa malformations variably involving the vermis, the fourth ventricle, and the cisterna magna may resemble each other and distinguishing different diagnoses based on the imaging patterns is not always straightforward (Table 1). Second, until recently, not only embryological uncertainties but also terms like Dandy-Walker variant or Dandy-Walker spectrum have led to an inconsistent and sometimes confusing nomenclature. Generally, a detailed description is to be preferred over unspecific terminology and the main focus should be on the brain parenchyma rather than on cystoid components. Phase-contrast cine imaging for CSF flow evaluation may potentially enhance the specificity of MRI in the differentiation of posterior fossa malformations.

The genetic literature has further enriched the understanding of hindbrain development. Therefore, it is now known that cerebellar and posterior skull development are linked through inductive interactions between the mesenchyme and rhombic lip; however, cerebellar malformations may be imitated by imaging patterns attributable to

hemorrhagic, ischemic, or infectious disruptions. Congenital and postnatally developing hydrocephalus has to be appreciated for diagnostic, prognostic, and management reasons. It is a typical finding in BPC, frequently associated with cerebellar disruptions and DWM, and a rare complication of posterior fossa AC. On the other hand, the diagnosis of MCM or primary CH has to be questioned if associated with hydrocephalus.

Establishing accurate diagnoses is especially critical in the context of fetomaternal medicine. Delayed vermian rotation, for example, may be an imaging pitfall demanding follow-up in the early third trimester to confirm persistent BP versus VH or DWM. The cerebellar "tail sign" in association with vermian hypoplasia/dysplasia should not be viewed as a specific imaging marker for DWM since a similar pattern may be distinguished in second trimester MRI of delayed BP rupture. Magnetic resonance imaging has gained acceptance as a potential problem solver in fetal neuroimaging and scanning at field strengths up to 3 T is believed to be safe within specific absorption rate limits.

Compliance with ethical guidelines

Conflict of interest T. Kau, R. Marterer, R. Kottke, R. Birnbacher, J. Gellen, E. Nagy and E. Boltshauser declare that they have no competing interests.

Ethical standards All investigations described in this manuscript were carried out with the approval of the responsible ethics committee and in accordance with national law and the Helsinki Declaration of 1975 (in its current revised form). Informed consent was obtained from patients if identifiable from images or other information within the manuscript. In the case of underage patients informed consent was obtained from the legal representatives.

References

1. Gandolfi Colleoni G, Contro E, Carletti A, Ghi T, Campobasso G, Rembouskos G, Volpe G, Pilu G, Volpe P. Prenatal diagnosis and outcome of fetal posterior fossa fluid collections. Ultrasound Obstet Gynecol. 2012;39:625–31.
2. Doherty D, Millen KJ, Barkovich AJ. Midbrain and hindbrain malformations: advances in clinical diagnosis, imaging, and genetics. Lancet Neurol. 2013;12:381–93.
3. Tortori-Donati P, Fondelli MP, Rossi A, Carini S. Cystic malformations of the posterior cranial fossa originating from a defect of the posterior membranous area, mega cisterna magna and persisting Blake's pouch: two separate entities. Childs Nerv Syst. 1996;12:303–8.
4. Blake JA. The roof and lateral recesses of the fourth ventricle, considered morphologically and embryologically. J Comp Neurol. 1900;10:79–108.
5. Yildiz H, Yazici Z, Hakyemez B, Erdogan C, Parlak M. Evaluation of CSF flow patterns of posterior fossa cystic malformations using CSF flow MR imaging. Neuroradiology. 2006;48:595–605.
6. Mohammad SA, Osman NM, Ahmed KA. The value of CSF flow studies in the management of CSF disorders in children: a pictorial review. Insights Imaging. 2019;10:3.
7. Paladini D, Donarini G, Parodi S, Volpe G, Sglavo G, Fulcheri E. Hindbrain morphometry and choroid plexus position in differential diagnosis of posterior fossa cystic malformations. Ultrasound Obstet Gynecol. 2019;54:207–14.
8. Huisman TAGM, Poretti A. Disorders of brain development. In: Atlas SW, editor. Magnetic resonance imaging of the brain and spine. 5th ed. Philadelphia: Wolters Kluver; 2017. pp. 116–22.
9. Nelson MD Jr, Maher K, Gilles FH. A different approach to cysts of the posterior fossa. Pediatr Radiol. 2004;34:720–32.
10. Robinson AJ. Inferior vermian hypoplasia—preconception, misconception. Ultrasound Obstet Gynecol. 2014;43:123–36.
11. Calabrò F, Arcuri T, Jinkins JR. Blake's pouch cyst: an entity within the Dandy-Walker continuum. Neuroradiology. 2000;42:290–5.
12. Kau T, Birnbacher R, Schwärzler P, Habernig S, Deutschmann H, Boltshauser E. Delayed fenestration of Blake's pouch with or without vermian hypoplasia: fetal MRI at 3 tesla versus 1.5 tesla. Cerebellum Ataxias. 2019;6:4.
13. Pinto J, Paladini D, Severino M, Morana G, Pais R, Martinetti C, Rossi A. Delayed rotation of the cerebellar vermis: a pitfall in early second-trimester fetal magnetic resonance imaging. Ultrasound Obstet Gynecol. 2016;48:121–4.
14. Bontognali M, Poretti A, Guzman R, Huisman TA, Ramelli GP. Blake's pouch cyst in children: Atypical clinical presentation. Neuroradiol J. 2018;31:430–3.
15. Cornips EM, Overvliet GM, Weber JW, Postma AA, Hoeberigs CM, Baldewijns MM, Vles JS. The clinical spectrum of Blake's pouch cyst: report of six illustrative cases. Childs Nerv Syst. 2010;26:1057–64.
16. Hirono S1, Ito D, Murai H, Kobayashi M, Suyama M, Fujii K, Saeki N. Postnatal development of Blake's pouch cyst: a case report and new insight for ist pathogenesis. Childs Nerv Syst. 2014;30:1767–71.
17. Brusius CV, Cavalheiro S. Endoscopic third ventriculostomy is a safe and effective procedure for the treatment of Blake's pouch cyst. Arq Neuropsiquiatr. 2013;71:545–8.
18. Boltshauser E, Martin F, Altermatt S. Outcome in children with space-occupying posterior fossa arachnoid cysts. Neuropediatrics. 2002;33:118–21.
19. De Keersmaecker B, Ramaekers P, Claus F, Witters I, Ortibus E, Naulaers G, Van Calenbergh F, De Catte L. Outcome of 12 antenatally diagnosed fetal arachnoid cysts: case series and review of the literature. Eur J Paediatr Neurol. 2015;19:114–21.
20. Catala M. The cerebellum and its wrapping meninge: developmental interplay between two major structures. Neuropediatrics. 2017;48:329–39.
21. Aldinger KA, Lehmann OJ, Hudgins L, Chizhikov VV, Bassuk AG, Ades LC, Krantz ID, Dobyns WB, Millen KJ. FOXC1 is required for normal cerebellar development and is a major contributor to chromosome 6p25.3 Dandy-Walker malformation. Nat Genet. 2009;41:1037–42.
22. Parrini E, Ramazzotti A, Dobyns WB, Mei D, Moro F, Veggiotti P, Marini C, Brilstra EH, Dalla Bernardina B, Goodwin L, Bodell A, Jones MC, Nangeroni M, Palmeri S, Said E, Sander JW, Striano P, Takahashi Y, Van Maldergem L, Leonardi G, Wright M, Walsh CA, Guerrini R. Periventricular heterotopia: phenotypic heterogeneity and correlation with Filamin A mutations. Brain. 2006;129:1892–906.
23. Lange M, Kasper B, Bohring A, Rutsch F, Kluger G, Hoffjan S, Spranger S, Behnecke A, Ferbert A, Hahn A, Oehl-Jaschkowitz B, Graul-Neumann L, Diepold K, Schreyer I, Bernhard MK, Mueller F, Siebers-Renelt U, Beleza-Meireles A, Uyanik G, Janssens S, Boltshauser E, Winkler J, Schuierer G, Hehr U. 47 patients with FLNA associated periventricular nodular heterotopia. Orphanet J Rare Dis. 2015;10:134.
24. Poretti A, Boltshauser E. Terminology in morphological anomalies of the cerebellum does matter. Cerebellum ataxias. 2015;2:8.

25. Ber R, Bar-Yosef O, Hoffmann C, Shashar D, Achiron R, Katorza E. Normal fetal posterior fossa in MR imaging: new biometric data and possible clinical significance. AJNR Am J Neuroradiol. 2015;36:795–802.
26. Katorza E, Bertucci E, Perlman S, Taschini S, Ber R, Gilboa Y, Mazza V, Achiron R. Development of the fetal vermis: new biometry reference data and comparison of 3 diagnostic modalities-3D ultrasound, 2D ultrasound, and MR imaging. AJNR Am J Neuroradiol. 2016;37:1359–66.
27. Jandeaux C, Kuchcinski G, Ternynck C, Riquet A, Leclerc X, Pruvo JP, Soto-Ares G. Biometry of the cerebellar vermis and brain stem in children: MR imaging reference data from measurements in 718 children. AJNR Am J Neuroradiol. 2019;40:1835–41.
28. Poretti A, Boltshauser E, Huisman TAGM. Pre- and postnatal neuroimaging of congenital cerebellar abnormalities. Cerebellum. 2016;15:5–9.
29. Siegel DH. PHACE syndrome: Infantile hemangiomas associated with multiple congenital anomalies: clues to the cause. Am J Med Genet C Semin Med Genet. 2018;178:407–13.
30. Poretti A, Boltshauser E, Doherty D. Cerebellar hypoplasia: differential diagnosis and diagnostic approach. Am J Med Genet C Semin Med Genet. 2014;166C:211–26.
31. Leibovitz Z, Guibaud L, Garel C, Massoud M, Karl K, Malinger G, Haratz KK, Gindes L, Tamarkin M, Ben-Sira L, Lev D, Shalev J, Brasseur-Daudruy M, Contreras Gutierrez de Piñeres CA, Lerman-Sagie T. The cerebellar "tilted telephone receiver sign" enables prenatal diagnosis of PHACES syndrome. Eur J Paediatr Neurol. 2018;22:900–9.
32. Poretti A, Boltshauser E, Valente EM. The molar tooth sign is pathognomonic for Joubert syndrome! Pediatr Neurol. 2014;50: e15–e6.
33. Poretti A, Snow J, Summers AC, Tekes A, Huisman TAGM, Aygun N, Carson KA, Doherty D, Parisi MA, Toro C, Yildirimli D, Vemulapalli M, Mullikin JC; NISC Comparative Sequencing Program, Cullinane AR, Vilboux T, Gahl WA, Gunay-Aygun M. Joubert syndrome: neuroimaging findings in 110 patients in correlation with cognitive function and genetic cause. J Med Genet. 2017;54:521–9.
34. Romaniello R, Arrigoni F, Panzeri E, Poretti A, Micalizzi A, Citterio A, Bedeschi MF, Berardinelli A, Cusmai R, D'Arrigo S, Ferraris A, Hackenberg A, Kuechler A, Mancardi M, Nuovo S, Oehl-Jaschkowitz B, Rossi A, Signorini S, Tüttelmann F, Wahl D, Hehr U, Boltshauser E, Bassi MT, Valente EM, Borgatti R. Tubulin-related cerebellar dysplasia: definition of a distinct pattern of cerebellar malformation. Eur Radiol. 2017;27:5080–92.
35. D'Antonio F, Khalil A, Garel C, Pilu G, Rizzo G, Lerman-Sagie T, Bhide A, Thilaganathan B, Manzoli L, Papageorghiou AT. Systematic review and meta-analysis of isolated posterior fossa malformations on prenatal ultrasound imaging (part 1): nomenclature, diagnostic accuracy and associated anomalies. Ultrasound Obstet Gynecol. 2016;47:690–7.
36. Limperopoulos C, Robertson RL, Estroff JA, Barnewolt C, Levine D, Bassan H, du Plessis AJ. Diagnosis of inferior vermian hypoplasia by fetal magnetic resonance imaging: potential pitfalls and neurodevelopmental outcome. Am J Obstet Gynecol. 2006;194:1070–6.
37. Dandy WE, Blackfan KD. Internal hydrocephalus: an experimental, clinical and pathological study. Am J Dis Child. 1914;8:406–82.
38. Robinson AJ. Posterior fossa anomalies. In: Kline-Faith BM, Bulas DI, Bahado-Singh R, editors. Fetal imaging—ultrasound and MRI. Philadelphia: Wolters Kluwer; 2015. pp. 430–53.
39. Barkovich AJ, Millen KJ, Dobyns WB. A developmental and genetic classification for midbrain-hindbrain malformations. Brain. 2009;132:3199–230.
40. Haldipur P, Dang D, Aldinger KA, Janson OK, Guimiot F, Adle-Biasette H, Dobyns WB, Siebert JR, Russo R, Millen KJ. Phenotypic outcomes in mouse and human Foxc1 dependent dandy-walker cerebellar malformation suggest shared mechanisms. Elife. 2017 Jan 16;6. https://doi.org/10.7554/eLife.20898.
41. Aldinger KA, Timms AE, Thomson Z, Mirzaa GM, Bennett JT, Rosenberg AB, Roco CM, Hirano M, Abidi F, Haldipur P, Cheng CV, Collins S, Park K, Zeiger J, Overmann LM, Alkuraya FS, Biesecker LG, Braddock SR, Cathey S, Cho MT, Chung BHY, Everman DB, Zarate YA, Jones JR, Schwartz CE, Goldstein A, Hopkin RJ, Krantz ID, Ladda RL, Leppig KA, McGillivray BC, Sell S, Wusik K, Gleeson JG, Nickerson DA, Bamshad MJ, Gerrelli D, Lisgo SN, Seelig G, Ishak GE, Barkovich AJ, Curry CJ, Glass IA, Millen KJ, Doherty D, Dobyns WB. Redefining the etiologic landscape of cerebellar malformations. Am J Hum Genet. 2019;105:606–15.
42. Bernardo S, Vinci V, Saldari M, Servadei F, Silvestri E, Giancotti A, Aliberti C, Porpora MG, Triulzi F, Rizzo G, Catalano C, Manganaro L. Dandy-Walker malformation: is the 'tail sign' the key sign? Prenat Diagn. 2015;35:1358–64.
43. Brodal A, Hauglie-Hanssen E. Congenital hydrocephalus with defective development of the cerebellar vermis (Dandy-Walker syndrome) clinical and anatomical findings in two cases with particular reference to the so-called atresia of the foramina of Magendie and Luschka. J Neurol Neurosurg Psychiatry. 1959;22:99–108.
44. Volpe P, Contro E, De Musso F, Ghi T, Farina A, Tempesta A, Volpe G, Rizzo N, Pilu G. Brainstem-vermis and brainstem-tentorium angles allow accurate categorization of fetal upward rotation of cerebellar vermis. Ultrasound Obstet Gynecol. 2012;39:632–5.
45. Kollias SS, Ball WS Jr, Prenger EC. Cystic malformations of the posterior fossa: differential diagnosis clarified through embryologic analysis. Radiographics. 1993;13:121–31.
46. Wüest A, Surbek D, Wiest R, Weisstanner C, Bonel H, Steinlin M, Raio L, Tutschek B. Enlarged posterior fossa on prenatal imaging: differential diagnosis, associated anomalies and postnatal outcome. Acta Obstet Gynecol Scand. 2017;96:837–43.
47. Boddaert N, Klein O, Ferguson N, Sonigo P, Parisot D, Hertz-Pannier L, Baraton J, Emond S, Simon I, Chigot V, Schmit P, Pierre-Kahn A, Brunelle F. Intellectual prognosis of the Dandy-Walker malformation in children: the importance of vermian lobulation. Neuroradiology. 2003;45:320–4.
48. Martino F, Malova M, Cesaretti C, Parazzini C, Doneda C, Ramenghi LA, Rossi A, Righini A. Prenatal MR imaging features of isolated cerebellar haemorrhagic lesions. Eur Radiol. 2016;26:2685–96.
49. Messerschmidt A, Brugger PC, Boltshauser E, Zoder G, Sterniste W, Birnbacher R, Prayer D. Disruption of cerebellar development: potential complication of extreme prematurity. AJNR Am J Neuroradiol. 2005;26:1659–67.
50. Limperopoulos C, Folkerth R, Barnewolt CE, Connolly S, Du Plessis AJ. Posthemorrhagic cerebellar disruption mimicking Dandy-Walker malformation: fetal imaging and neuropathology findings. Semin Pediatr Neurol. 2010;17:75–81.
51. Volpe JJ. Cerebellum of the premature infant: rapidly developing, vulnerable, clinically important. J Child Neurol. 2009;24:1085–104.
52. Bosemani T, Orman G, Boltshauser E, Tekes A, Huisman TA, Poretti A. Congenital abnormalities of the posterior fossa. Radiographics. 2015;35:200–20.